

The Use of Ultrasound to Measure Dislocation Density

FELIPE BARRA,¹ RODRIGO ESPINOZA-GONZÁLEZ,²
HENRY FERNÁNDEZ,¹ FERNANDO LUND,^{1,5} AGNES MAUREL,³
and VINCENT PAGNEUX⁴

1.—Departamento de Física and CIMAT, Facultad de Ciencias Físicas y Matemáticas, Universidad de Chile, Santiago, Chile. 2.— Departamento de Ciencia de los Materiales, Facultad de Ciencias Físicas y Matemáticas, Universidad de Chile, Santiago, Chile. 3.— Institut Langevin, ESPCI, 1 rue Jussieu, Paris 75005, France. 4.— LAUM, UMR CNRS 6613, Av. O. Messiaen, 72085 Le Mans Cedex 9, France. 5.—e-mail: flund@cimat.cl

Dislocations are at the heart of the plastic behavior of materials yet they are very difficult to probe experimentally. Lack of a practical nonintrusive measuring tool for, say, dislocation density, seriously hampers modeling efforts, as there is little guidance from data in the form of quantitative measurements, as opposed to visualizations. Dislocation density can be measured using transmission electron microscopy (TEM) and x-ray diffraction (XRD). TEM can directly show the strain field around dislocations, which allows for the counting of the number of dislocations in a micrograph. This procedure is very laborious and local, since samples have to be very small and thin, and is difficult to apply when dislocation densities are high. XRD relies on the broadening of diffraction peaks induced by the loss of crystalline order induced by the dislocations. This broadening can be very small, and finding the dislocation density involves unknown parameters that have to be fitted with the data. Both methods, but especially TEM, are intrusive, in the sense that samples must be especially treated, mechanically and chemically. A nonintrusive method to measure dislocation density would be desirable. This paper reviews recent developments in the theoretical treatment of the interaction of an elastic wave with dislocations that have led to formulae that relate dislocation density to quantities that can be measured with samples of cm size. Experimental results that use resonant ultrasound spectroscopy supporting this assertion are reported, and the outlook for the development of a practical, nonintrusive, method to measure dislocation density is discussed.

DISLOCATIONS MATTER: WHY?

Dislocations are line defects in a crystalline material. Their existence explains why the experimental value of the shear stress needed to plastically deform a crystal is several orders of magnitude less than the theoretical value, obtained on the basis of the shear stress needed to rigidly slide one atomic plane past an adjacent one. They are thus the basic building block of our current understanding of the plastic behavior of materials.¹ Now, suppose you have a piece of metal: how can you know the number and position of dislocations? There are a number of situations where this question is critically important.

Ductile to Brittle Transition²

When loaded in tension, some materials will break without previous deformation, i.e., will undergo brittle fracture characterized by the sudden propagation of a crack, while others will first deform, because of a large proliferation of dislocations, and only then will fail: they undergo ductile failure. Interestingly, some materials, for example bcc metals such as low carbon steels may present different behaviors depending on temperature: brittle at low temperatures, and ductile at high. There is a transition, which can be more or less abrupt, at a “transition temperature”. The factors that determine this ductile to brittle transition

temperature (DBTT) are largely unknown at a quantitative level, although they relate to a critical property of structural materials. Additional factors that matter include the strain rate and impurity content.

Fatigue³

Materials cyclically loaded can fail after many cycles, even though the amplitude of the load can be thought of as very low in a static test. The generation of (micro)cracks, and their subsequent evolution, including the effect of plasticity, has been the object of extensive experimental research, for which there exists very little modeling with quantitative predictive power. Do microcracks initially coalesce from dislocation pile-ups? If so, how? Do dislocations nucleate from a crack tip? At what rate? How is the ensuing crack dynamics affected? These are examples of questions that probe the limits of the fundamental understanding of fatigue.

Radiation Damage^{4,5}

Neutron radiation of zirconium and its alloys, widely used in nuclear power plants, generates dislocation loops. Their nucleation, growth and interaction with other defects have been studied for decades because of the possible physical threats to materials caused by radiation damage, such as embrittlement, swelling and creep. Nevertheless, it does not seem unfair to say that quantitative modeling of these phenomena could greatly be advanced by data obtained nonintrusively.^{6,7}

Pattern Formation and Material Instabilities

Sometimes, dislocations arrange themselves in patterns that may lead to undesired effects for a material in service. For example, Al-Mg alloys for the automotive industry are prone to the Portevin–Le Châtelier effect,^{8,9} which generates stretcher lines on the aluminum alloys sheets: under certain regimes of strain rate and temperature, plastic strain becomes localized in the form of bands. In addition to cosmetic problems, this can also lead to structural problems: embrittlement can be increased and fracture toughness decreased, leading to unexpected failure. Why does this effect happen? Is it possible to control it?

DISLOCATION DENSITY: WHAT IS KNOWN AND WHAT ONE WOULD LIKE TO KNOW

Dislocations are line defects within a crystalline structure, and their motion through the crystal lattice is the major source for plastic deformation at room temperature. Their influence on the properties of a given material, particularly mechanical, are most significant when they appear, as they often do, in large numbers. Thus, a natural approach to develop quantitative modeling is to introduce a length scale, intermediate between the interatomic

spacing and the sample size (the “mesoscale”), where there are still many dislocations, and to define the *dislocation density* as the total length of dislocation contained within a given volume, divided by said volume. The units of dislocation density are thus inverse length squared, or m^{-2} , and it is, in general, a function of position at the intermediate length scale. The theoretical framework is continuum mechanics.

Dislocation density is a critical variable that determines dislocation mobility, and the strength and ductility of materials. As such, it has long been the object of much modeling and analysis. An inroad into the vast literature is provided by the recent publications of Arsenlis et al.,¹⁰ Lee et al.,¹¹ and Leung et al.,¹² A recurrent theme appears to be that, although dislocation density is a variable that figures prominently in the model building, it is a variable that is most often probed only indirectly through the consequences it has on standard mechanical tests. A direct way to measure dislocation density would surely add considerable depth to any modeling of plastic behavior. Now, although individual dislocations can be studied in detail using transmission electron microscopy, their collective behavior is much harder to probe.

Standard Methods to Measure Dislocation Density

Transmission electron microscopy (TEM) and x-ray diffraction (XRD) are two complementary techniques strongly developed in the previous century that use the diffraction of waves to visualize the structure of matter. Both techniques work similarly: whereas XRD uses x-ray radiation, TEM uses the wave behavior of electrons that can be diffracted by an array of atoms. Nevertheless, the distinct degree of interaction with matter produces different levels of information that can be obtained from each technique.

TEM

In conventional TEM, individual dislocations, or groups thereof, are revealed by the strain of the lattice around the core line, which produces a distinctive diffraction contrast due to the local displacement of the planes. Under proper conditions, the dislocations appear as a narrow line of opposite contrast to the surrounded matrix in a TEM image (see Fig. 1). This makes it possible to account for the local density of dislocations with high precision and to determine structural parameters such as the Burgers vector, the dislocation character and the glide plane.¹³

TEM can also reveal the local atomic structure down to individual lattice sites, which has been the most remarkable development of the last decades. The first atomic arrays and individual dislocations in an interface were visualized at the beginning of the 1980s.^{14,15} During the following decades, the

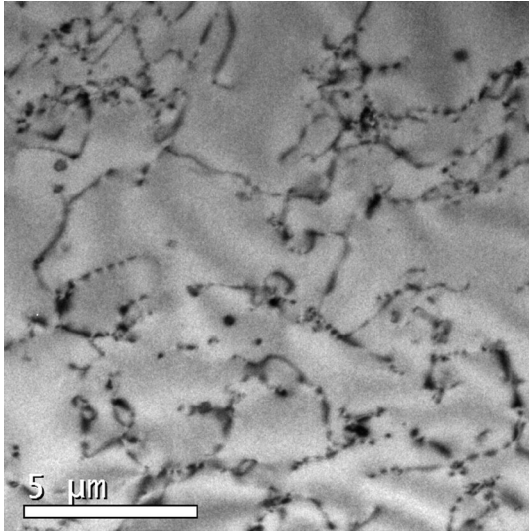


Fig. 1. TEM image of the strain field of dislocations in an aluminum 1100 (99.0% pure) sample annealed at 673 K for 10 h..

correction of lens aberration in the optical system of electron microscopes have allowed sub-Ångström imaging of atomic arrangement.¹⁶ The TEM ability to visualize individual dislocations has been used, notably, to directly observe dislocation motion under tensile loading in the microscope, to elucidate high-temperature plastic deformation mechanisms in materials,¹⁷ and for the detailed study of planar defects such as stacking faults and the interaction of twin boundaries in nanotwinned films.¹⁸

Despite all the valuable information that can be obtained from the atomic structure of, and interfaces between, different materials by TEM, an important consideration that must be kept in mind is that this information comes from a very small portion of material. The TEM sample has to be very thin to be transparent to the electron beam, which limits the visual field to a few micrometers under the best of circumstances. Consequently, the determination of dislocation density in a reliable way from a piece of material has always been a limitation of TEM, because it involves many measurements in order to have a statistically representative value.¹⁹ Additionally, in highly deformed materials where the dislocation density is high, the interaction between the strain fields of the dislocations make it very difficult to distinguish between individual dislocations, limiting the applicability of this technique. Furthermore, the preparation of TEM samples from the bulk part of interest is necessarily destructive, leading to the question whether the dislocations are affected during the preparation procedure.

XRD

X-rays interact relatively weakly with matter, which implies that they can penetrate several millimeters of material, but their spatial resolution is

low (typically several micrometers). X-rays are therefore sensitive to long-range features, average crystal structures, and average deviations from long-range order, especially lattice strains and stresses. In this sense, XRD has a better capacity to measure the dislocation density in bulk samples than TEM, but is still limited to a specially prepared sample normally cut from the main piece. The interaction of an x-ray beam with a perfect coherent domain of crystals produces a diffracted beam in a certain condition described by Bragg's equation. A single diffracted peak consists in several intensities I_i measured at several angles $2\theta_i$ distributed around a maximum intensity at a certain Bragg angle. The analysis of the diffracted peak consists in the adjustment to the measurement of a theoretical model that adjusts the microstructural factors. Among them, the most relevant are the dislocation density that produces the lattice strain and the crystallite size or coherent domain size.

The distortion in the interplanar distances of the crystal lattice produced by a dislocation is observed as a peak broadening in the x-ray diffractogram, which can be related to the strain field caused by dislocations.²⁰ The root-mean-square value of the total strain ϵ_{rms} is described in terms of the microstructural parameters by the relationship

$$\epsilon_{rms} = b \sqrt{\frac{\pi A \rho}{2}}, \quad (1)$$

where b is the modulus of the Burgers vector, A is a constant that depends on the effective cut off radius of the strain field caused by a dislocation, and ρ is the dislocation density in the coherent domain.²¹

The kinematical theory of XRD states that it is possible to separate the effect of the crystal domain size and of the lattice distortion effect from the peak profile analysis. The classical Williamson–Hall method allows for the determination of the crystallite size D , and strain ϵ_{rms} , separately from the adjustment of the coefficients of a linear fit.²² Modifications to this model have been proposed to give an account of the dislocation density considering the distortion of the lattice in the different crystallographic planes,^{23–25} which has been used in the study of processed deformed pure metals and alloys, e.g., equal channel angular pressing (ECAP) and cold-rolling.^{26,51} Compared to TEM, XRD microstructural analyses can be performed over a wide range of samples of different morphologies, e.g., bulk polycrystals, deposited thin films, nanocrystalline powders and powder of microscopic single crystals. Regarding the penetration of x-rays and the lower manipulation of the samples prior to the measurements, dislocation density obtained by XRD is a more representative quantity than the values obtained from TEM. According to Ungár,²⁷ currently available x-ray diffraction techniques allow access to dislocation densities as low as 100 m^{-2} and as high as 10^{18} m^{-2} . Due to the capabilities of

conventional diffractometers, samples of significant size can be measured where the quantitative results of the microstructural parameters are representative of a large volume size, from 1 up to 10 mm³. Nevertheless, some limitations of measurable crystallite size must be considered, related to the precision of the diffractometer goniometer.

ULTRASOUND

Ultrasound is widely used as a non-destructive testing tool. The reason is that acoustic waves can penetrate deep into a material. In addition, the energy they carry can be small enough not to disturb the material at hand, and yet provide a signal when it is scattered by a flaw or inhomogeneity in an otherwise homogeneous material (Fig. 2). Finally, the apparatus that is used can often be employed not only in the laboratory but also in the field and with pieces in service. Cracks, voids and bubbles are examples of inhomogeneities that are routinely diagnosed with ultrasonic techniques. If the scatterer is rigid, the scattering will be determined, to a first approximation, by the impedance mismatch and the ratio between object size and wavelength. If the scatterer, however, can be deformed, it will have, in general, a number of resonant frequencies. Tuning the acoustic frequencies to these eigenfrequencies can greatly increase the scattered signal.

The question arises: would it be possible to use ultrasound to monitor the presence—or absence—of dislocations? For this idea to work, dislocations would have to scatter sound, and we now turn our attention to this question.

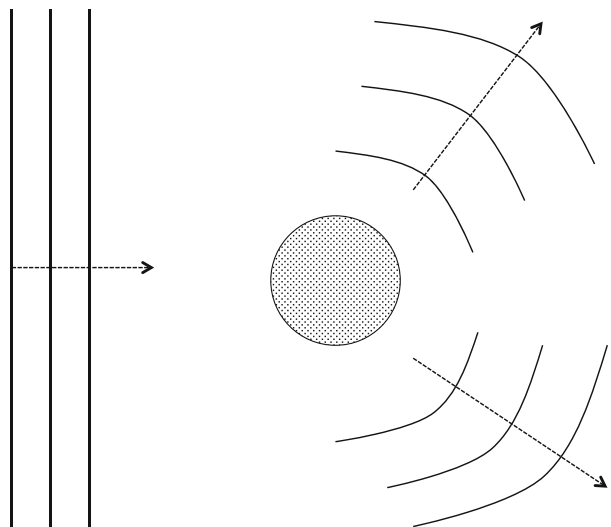


Fig. 2. Flaws, voids, bubbles and inhomogeneities, in general in an otherwise homogeneous material, scatter sound. This is due to the impedance mismatch between the two materials. The monitoring of the scattered wave provides information about, to start with, the presence or absence of the inhomogeneity. Further treatment can provide additional information about number, shape, distribution and character.

Why Should Dislocations Scatter Sound?

The fact that dislocations should scatter sound was realized by Nabarro²⁸ and Eshelby^{29,30} on the basis of an analogy between elastic waves in interaction with dislocations on the one hand, and electromagnetic waves in interaction with electrons on the other. To see this, think of the way x-rays interact with matter: an incoming electromagnetic wave hits an electron which oscillates in response; as it oscillates, the electron generates secondary, i.e., scattered electromagnetic waves. The reason that this process, under the name x-ray diffraction, is so useful as a materials characterization tool is because, when many electrons are present, the scattered wave carries information about the scatterer position.

Similarly, an incoming elastic wave that hits a dislocation will cause it to oscillate in response and, as it does, will generate secondary, scattered, elastic waves (Fig. 3). However, the electromagnetic analogy of Nabarro and Eshelby, while providing a powerful picture to reason by analogy, could only be translated into precise mathematical statements in the case of screw dislocations in interaction with anti-plane shear waves in two dimensions.

In the general three-dimensional case, a number of difficulties have to be dealt with as elastic waves have three polarizations (acoustics being the longitudinal one). Their propagation in a crystal is determined by the anisotropy of the material whose elastic properties are determined by, in the most general case, 21 elastic constants. When the material can be considered isotropic to a good approximation, only two constants remain and waves have two speeds of propagation, one for acoustic and the other for shear waves. In addition, it must be

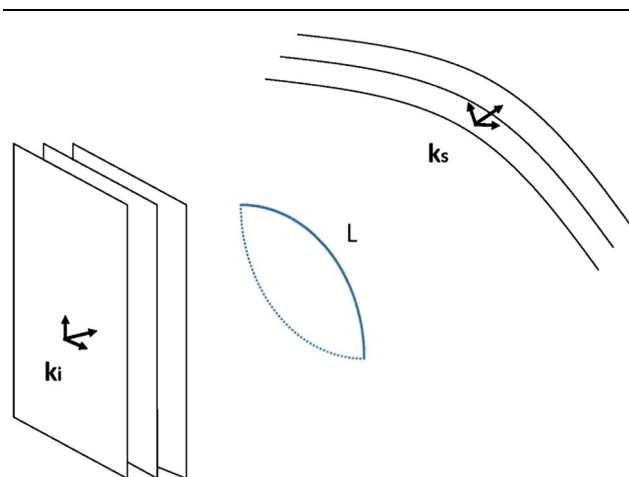


Fig. 3. The basic scattering mechanism of sound by a vibrating dislocation: a plane wave, which can have both longitudinal and transverse components, with incident wave vector k_i hits a dislocation segment of length L . This segment is characterized not only by this length but also by its orientation, and by the orientation of its Burgers vector. In response to the incident wave, the dislocation oscillates and, as it does, generates secondary scattered waves characterized by a scattered wave vector k_s .

remembered that a dislocation is a line, in general a closed curve, whose length need not be small compared with an acoustic wavelength, and is endowed with a property, called the Burgers vector, that must also be taken into account. These difficulties were overcome in the isotropic case by Mura³¹ and by Lund,³² who gave complete formulations for the emission of elastic waves by a dislocation loop in arbitrary motion, and for the response of a dislocation loop of arbitrary shape to an incoming plane wave, respectively.

Granato-Lücke Theory: Strengths and Limitations

In the 1950s, Granato and Lücke^{33,34} developed a theory of mechanical damping and modulus change due to dislocations which are both frequency- and strain amplitude-dependent. This theory considered a stress wave that travels through a solid which contains pinned dislocations of length L with a total length Λ of movable dislocation line per unit volume. Introducing a length scale, given by L , naturally leads to a frequency-dependent (or wavelength-dependent) attenuation and wave velocity. By allowing, in addition, for the possibility of the dislocations to break away from their pinning points, the theory could account for the amplitude dependence of losses. This model has been enormously successful and to this day is the standard tool to interpret many experimental results. However, as experiments have become more precise, its limitations have become apparent, and efforts to use it, for example, to understand thermal conductivity properties, have been largely unsuccessful.³⁵ From a conceptual point of view, limitations include a number of technical assumptions, for example about the relative orientations of the various dislocation segments. These assumptions have little qualitative consequences, but do have quantitative consequences. More broadly, the theory cannot distinguish between acoustic and shear waves, or between edge and screw dislocations.

Recent Developments

In recent years, Maurel et al.^{36–47} have revisited the issue of the interaction between elastic wave and dislocations. They took full account of the vector nature of this problem and used multiple scattering theory. This section reviews these developments and how they have led to a reasonable tool to measure dislocation density.

Ultrasonic frequencies are in the range of tens of KHz to hundreds of MHz. For most materials, this means wavelengths in the range of tens of cm to tens of microns, safely larger than dislocation length and inter-dislocation distance for many situations of interest.

Scattering by an Isolated Dislocation Segment

The basic scattering mechanism of sound by dislocations is shown in Fig. 3. An incoming wave hits a dislocation that oscillates in response and, as it does, generates secondary, scattered, waves. How efficient can this process be? How much energy, say, does a pinned edge dislocation segment take away from an incoming plane wave? Quite generally, in any scattering process, this is measured by the scattering cross-section σ , which is the ratio of the total energy radiated away as secondary waves to the energy per unit surface which is brought in by the incoming plane wave:

$$\sigma = \frac{(\text{Total energy scattered away})}{(\text{Incoming energy/area})}. \quad (2)$$

The scattering cross-section σ has units of surface.

The scattering cross-section for an acoustic wave of wavelength λ by an otherwise isolated dislocation of length L , in the limit $\lambda \gg L$ that will hold for ultrasound, averaged over all possible orientations, is³⁹

$$\sigma = aL^2 \left(\frac{L}{\lambda} \right)^4, \quad (3)$$

with $a = 10/(3^{7/2}\pi)$ for a Poisson solid. A single, isolated dislocation will generally produce an extremely small signal. Many dislocations, however, can collectively generate a detectable signal.

The Averaged Effect of Many Dislocations

When an elastic wave interacts with many dislocations, as in Fig. 4, computing the detailed wave behavior can be daunting. However, the interference pattern from all the multiple scattered waves can arrange itself, on average, into a coherently propagating result that, for propagation along the x

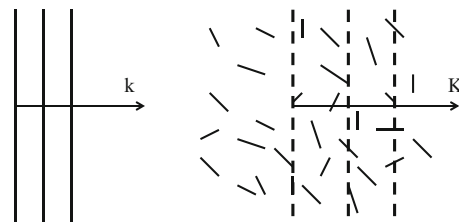


Fig. 4. In the absence of dislocations (*left*), and in an isotropic material, an elastic wave propagates with a wave vector $k_a = \omega/c_a$ with $a = L, T$ for longitudinal (L) or transverse (T) waves. In the presence of dislocations (*right*), the interference pattern of the multiple scattered wave arranges itself to give, on average, a coherently propagating wave with an “effective” wave vector K_a that is a complex quantity: the real part provides an effective phase velocity and the imaginary part provides an attenuation coefficient. The latter has two origins: from inner losses due to the viscous damping of the dislocation motion, and from the incoherently scattered energy away from the direction of incidence.

direction in time t , can be described as a damped harmonic wave of angular frequency ω :

$$U(x, t) = U_0 e^{-\alpha_a x} e^{i\omega(x/v_a - t)}. \quad (4)$$

Here, U_0 is an overall amplitude, α_a ($a = L, T$) is a damping coefficient and v_a is an effective speed of propagation. Both quantities are different for longitudinal (L) and transverse (T) waves. Their precise expressions as a function of frequency have been computed for a variety of dislocation arrangements by Maurel et al.⁴⁰

Of special interest, because of its simplicity both from an analytical and experimental point of view, is the low frequency limit $\omega \rightarrow 0$. In the following, we restrict ourselves to edge dislocations. Results for screws, as well as prismatic loops, are also available.⁴⁵

a. *Low frequency damping* At low frequencies, a remarkable result emerges:⁴⁰ the ratio of damping for longitudinal to transverse waves due to dislocations comes out to be independent of all aspects of the dislocation distribution for a given sample of material:

$$\frac{\alpha_T}{\alpha_L} = \frac{3c_L}{4c_T}, \quad (5)$$

where c_L (resp. c_T) is the speed of sound (resp. shear) waves in the absence of dislocations. This result provides an explanation for measurements with polycrystalline copper,⁴⁸ copper single crystals⁴⁹ and LiNbO_3 ⁵⁰ that it had not been possible to explain on the basis of the Granato-Lücke theory because it does not distinguish longitudinal and transverse polarizations.

b. *Velocity of propagation at low frequencies* Here, it turns out that the dislocations induce a change in the velocity of propagation both of longitudinal and of transverse waves. In the latter case, and for edge dislocations, it is⁴⁰

$$\frac{\Delta v_T}{c_T} = \frac{4}{5\pi^4} nL^3 \quad (6)$$

where $\Delta v_T = c_T - v_T$ is the difference between the speed of propagation c_T in the absence of dislocations and the speed of propagation v_T in the presence of dislocations, and n is the number of dislocation segments of length L per unit volume. The relationship of this quantity to the total length of dislocation per unit volume Λ is given by $\Lambda = nL$

Equation (6) relates a change in the speed of propagation of shear waves to the density of dislocations that is causing the change. So, if the velocity difference can be measured, a value for the dislocation density is obtained automatically. To get a feeling for the orders of magnitude involved, con-

sider a hypothetical dislocation density $\Lambda \sim 10^{14} \text{ m}^{-2}$ with length $L \sim 100 \text{ nm}$. This gives, according to (6), a fractional change in wave velocity at the 1% level, well within current experimental capabilities.

Resonant Ultrasound Spectroscopy

Relationship (6) has been tested with satisfactory results using resonant ultrasound spectroscopy (RUS) by Mujica et al.⁵¹ This is a technique that measures the resonance frequencies (i.e., the frequencies of the normal modes of vibration) of a sample of material.⁵² From these measurements and an independent measurement of the sample shape and density, the elastic moduli, and hence the elastic wave velocities, can be inferred.

What Mujica et al.⁵¹ did was to take a piece of commercially 1100 pure aluminum (99.0% pure) and cut it into five pieces. One was left as control, two were cold-rolled at either 33% or 43% of the initial diameter of the as-received material, and the other two were annealed at 673 K, one for 5 h and the other for 10 h. It is well known that longer annealing leads to lower dislocation density and stronger cold-rolling leads to higher dislocation density. The challenge is to turn these qualitative statements into quantitative ones. From each of the five pieces, presumably with different dislocation densities, one portion was set aside for RUS testing and a second for XRD. Figure 5 shows the results of measuring the speed of transverse waves using RUS and the dislocation density obtained with XRD using the Williamson-Hall plot mentioned in the

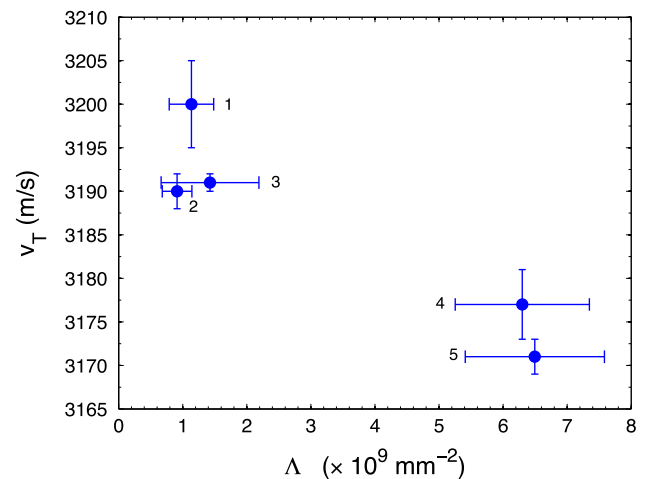


Fig. 5. RUS and XRD as tools to measure dislocation density compared and contrasted⁵¹: Sample 3 is the as-received material. Samples 1 and 2 were annealed at 673 K for 10 and 5 h, respectively. Samples 4 and 5 were cold-rolled at 33% and 43%, respectively. The *horizontal* axis shows the result obtained from the broadening of diffraction peaks induced by the presence of dislocations; it can distinguish two different densities within the five analyzed samples. The *vertical* axis is the respective speed of shear waves; it can distinguish four values within the same five samples. Equation (6) establishes the *difference* in dislocation density between the various samples.

“XRD” section. Of the five samples, RUS can distinguish four and XRD can distinguish two.

Equation (6) relates the difference in the speed of shear waves v_T to the the difference of dislocation density, defined as nL^3 , between two samples. Here, L is the average length of the dislocation segments between two pinning points that allow for string-like vibrations, as described in the “Why Should Dislocations Scatter Sound?” section, and n is the number of such segments per unit volume. Thus, nL^3 is dimensionless. This is a slightly different definition of dislocation density from the usual one, where dislocation density Λ is the ratio of total dislocation line length contained in a given volume divided by the said volume. Λ has dimensions of inverse surface (interpreted as the number of dislocation crossings of a surface per unit area). Both definitions can be related through $nL^3 = \Lambda L^2$. Applying these considerations to the data of Fig. 5 gives a difference between high and low values of $\Delta(nL^3) \sim 1$ and $\Delta\Lambda \sim 5 \times 10^9 \text{ mm}^{-2}$, yielding an average value for dislocation segment length between pinning points of $L \sim 10 - 20 \text{ nm}$, a not unreasonable value.

CONCLUSION AND OUTLOOK

Ultrasound interacts with dislocations, and this effect can be analyzed in great detail. It turns out that the interaction with a single dislocation is extremely weak, but, at the densities available in the plastic regime of many materials, dislocations collectively generate an effect that is measurable with current technology. This raises the hope for a non-intrusive characterization tool for the plastic behavior of materials which has significant advantages over current techniques such as XRD and TEM.

The hope has been fulfilled, as it has been established, using RUS, that ultrasound can be used to measure dislocation densities on the order of 10^{15} m^{-2} in the laboratory.⁵¹ The relative changes in the speed of shear waves these dislocations induce are at the level of 1%, in agreement with order of magnitude estimates obtained from the theoretical framework. These measurements have been obtained with a RUS apparatus that determines the wave velocity with an accuracy of 0.1%.

The experiment of Mujica et al.⁵¹ provides a proof-of-concept. Since ultrasonics is such a well-developed technology, and wave velocities can be measured with a high accuracy, a natural development should be to test these results in an environment that is still controlled, but is less artificial. For example, it should be interesting to monitor the speed of sound of a piece of metal undergoing a standard tension test. This could provide, in situ, a detailed picture of the evolution of dislocation density as a function of applied tension. A successful outcome of this test would be a significant step forward in the development of a practical and portable probe of dislocation density.

The theory reviewed in the “Recent Developments” section, and successfully tested by Mujica et al.,⁵¹ relies on the *linear* description of acoustic wave behavior, always valid for small enough wave amplitudes. However, it is comparatively easy with current technology to increase a signal to reach a *nonlinear* regime, where higher harmonic generation and resonance frequency shift are two striking and characteristic phenomena.⁵³ Indeed, nonlinear ultrasonic response has been shown to be a very sensitive probe in a number of situation.⁵⁴ Could nonlinear ultrasound resonance spectroscopy be a more sensitive tool to detect dislocation density than its linear counterpart? Quantitative analysis is here more involved, but preliminary results are encouraging.⁵⁵

Finally, the results quoted in the “Recent Developments” section deal with the coherent propagation of elastic waves in the presence of many dislocations in the low-frequency limit. There are at least two additional directions to move forward: (1) going to shorter wavelengths could provide a handle not only on the average dislocation length between pinning points but also on the statistical distribution of said lengths, and (2) a study of the incoherent wave propagation could lead to interesting insights into the role of dislocations on thermal conductivity.

ACKNOWLEDGEMENTS

We are grateful to A. Caro, M. Demkowicz, E. Donoso, D. Espíndola, C. Espinoza, N. Mujica, V. Salinas and A. Sepúlveda for useful discussions. We also acknowledge the support of Fondecyt Grant 1130382 and ANR-Conicyt Grant PROCOMEDIA.

REFERENCES

1. D. Hull and D. J. Bacon, *Introduction to Dislocations*, 5th edition (Elsevier, 2011).
2. G. Xu, *Dislocations in Solids*, eds. F.R.N. Nabarro and J.P. Hirth, vol. 12 (Elsevier, 2004).
3. U. Krupp, *Fatigue Crack Propagation in Metals and Alloys: Microstructural Aspects and Modelling Concepts* (Wiley, 2007).
4. G.S. Was, *Fundamentals of Radiation Materials Science* (Springer, Berlin, 2007).
5. S.J. Zinkle and G.S. Was, *Acta Mater.* 61, 735 (2013).
6. S.J. Zinkle and Y. Matsukawa, *J. Nucl. Mater.* 329–333, 88 (2004).
7. H. Wang, D.S. Xu, and R. Yang, *Model. Simul. Mater. Sci. Eng.* 22, 085004 (2014).
8. J. Coër, P.Y. Manach, H. Laurent, M.C. Oliveira, and L.F. Menezes, *Mech. Res. Commun.* 48, 1 (2013).
9. A. Yilmaz, *Sci. Technol. Adv. Mater.* 12, 063001 (16pp) (2011).
10. A. Arsenlis, D.M. Parks, R. Becker, and V.V. Bulatov, *J. Mech. Phys. Solids* 52, 1213 (2004).
11. M.G. Lee, H. Lim, B.L. Adams, J.P. Hirth, and R.H. Wagoner, *Int. J. Plasticity* 26, 925 (2010).
12. H.S. Leung, P.S.S. Leung, B. Cheng, and A.H.W. Ngan, *Int. J. Plasticity* 67, 1 (2015).
13. D. B. Williams and C. B. Carter, *Transmission Electron Microscopy*, 2nd Ed. (Springer, Berlin, 2009), Ch. 27.
14. F.A. Ponce, R. Sinclair, and R.H. Rube, *Appl. Phys. Lett.* 39, 951 (1981).
15. F.A. Ponce, T. Yamashita, and S. Hahn, *Appl. Phys. Lett.* 43, 1051 (1983).

16. P.E. Batson, N. Dellby, and O.L. Krivanek, *Nature* 418, 617 (2002).
17. S. Yamada and T. Sakai, *Microscopy* 63, 449 (2014).
18. N. Li, J. Wang, X. Zhang, and A. Misra, *J. Miner. Met. Mater. Soc.* 63, 62 (2011).
19. R.K. Ham, *Philos. Mag.* 6, 1183 (1961).
20. B. D. Cullity, *Elements of X-ray Diffraction*, 3rd edn. (Prentice Hall, 2001).
21. T. Ungár, *Appl. Phys. Lett.* 69, 3173 (1996).
22. G.K. Williamson and W.H. Hall, *Acta Metall.* 1, 22 (1953).
23. T. Ungár and A. Borbély, *Appl. Phys. Lett.* 69, 3173 (1996).
24. T. Ungár, I. Dragomir, A. Révész, and A. Borbély, *J. Appl. Cryst.* 32, 992 (1999).
25. T. Ungár and G. Tichy, *Phys. Stat. Sol. A* 171, 425 (1999).
26. M. R. Movaghar Garabagh, S. Hossein Nedjad, H. Shirazi, M. Iranpour Mobarekeh, and M. Nili Ahmadabadi, *Thin Solid Films* 516, 8117 (2008).
27. T. Ungár, *Mater. Sci. Eng. A* 309–310, 14 (2001).
28. F.R.N. Nabarro, *Proc. R. Soc. Lond. Ser. A* 209, 278 (1951).
29. J.D. Eshelby, *Proc. R. Soc. London, Ser. A* 197, 396 (1949).
30. J.D. Eshelby, *Phys. Rev.* 90, 248 (1953).
31. T. Mura, *Philos. Mag.* 8, 843 (1963).
32. F. Lund, *J. Mater. Res.* 3, 280 (1988).
33. A. Granato and K. Lücke, *J. Appl. Phys.* 27, 583 (1956).
34. A. Granato and K. Lücke, *J. Appl. Phys.* 27, 789 (1956).
35. G.A. Kneezel and A.V. Granato, *Phys. Rev. B* 25, 2851 (1982).
36. A. Maurel, J.-F. Mercier, and F. Lund, *J. Acoust. Soc. Am.* 115, 2773 (2004).
37. A. Maurel, J.-F. Mercier, and F. Lund, *Phys. Rev. B* 70, 024303 (2004).
38. A. Maurel, V. Pagneux, D. Boyer, and F. Lund, *Mater. Sci. Eng. A* 400–401, 222 (2005).
39. A. Maurel, V. Pagneux, F. Barra, and F. Lund, *Phys. Rev. B* 72, 174110 (2005).
40. A. Maurel, V. Pagneux, F. Barra, and F. Lund, *Phys. Rev. B* 72, 174111 (2005).
41. A. Maurel, V. Pagneux, D. Boyer, and F. Lund, *Proc. R. Soc. Lond. A* 462, 2607 (2006).
42. A. Maurel, V. Pagneux, F. Barra, and F. Lund, *J. Acoust. Soc. Am.* 121, 3418 (2007).
43. A. Maurel, V. Pagneux, F. Barra, and F. Lund, *Phys. Rev. B* 75, 224112 (2007).
44. A. Maurel, V. Pagneux, F. Barra, and F. Lund, *Int. J. Bifurc. Chaos* 19, 2765 (2009).
45. N. Rodriguez, A. Maurel, V. Pagneux, F. Barra, and F. Lund, *J. Appl. Phys.* 106, 054910 (2009).
46. A. Maurel, V. Pagneux, F. Barra, and F. Lund, *Phys. Rev. B* 80, 136102 (2009).
47. A. Maurel, V. Pagneux, F. Barra, and F. Lund, *Ultrasonics* 50, 161 (2010).
48. H.M. Ledbetter and C. Fortunko, *J. Mater. Res.* 10, 1352 (1995).
49. H. Ogi, H.M. Ledbetter, S. Kim, and M. Hirao, *J. Acoust. Soc. Am.* 106, 660 (1999).
50. H. Ogi, N. Nakamura, M. Hirao, and H. Ledbetter, *Ultrasonics* 42, 183 (2004).
51. N. Mujica, M.T. Cerda, R. Espinoza, J. Lisoni, and F. Lund, *Acta Mater.* 60, 5828 (2012).
52. A. Migliori and J. L. Sarrao, *Resonant Ultrasound Spectroscopy* (Wiley, New York, 1997).
53. L. D. Landau and I. M. Lifshitz, *Theory of Elasticity* (Pergamon, New York, 1970).
54. R. A. Guyer and P. A. Johnson, *Nonlinear Mesoscopic Elasticity: The Complex Behaviour of Rocks, Soil, Concrete* (Wiley, New York, 2009).
55. C. Espinoza, Magister thesis (U. de Chile, 2013).